Bachelor Thesis

The Phase Transition of DMPG and its Dependence on pH

Louise Revsbech Winther

May 2008

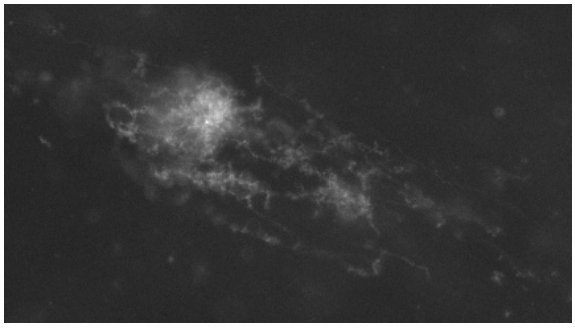

Niels Bohr Institute
Copenhagen University

Preface

The front page picture shows fluorescence microscopy of DMPG dispersions at 22°C.

Group leader, Prof. Thomas Heimburg
Supervisor

Acknowledgements

I would like to thank the members of the Membrane Biophysics Group at the Niels Bohr Institute for their help. In particular I would like to thank Andreas Blicher and Kaare Græsbøll for their help with Igor macros and dying computers. I thank Marie Domange Jordö for patiently introducing me to the techniques of fluorescence microscopy. Furthermore I would like to thank Kristmundur Sigmundsson and Kasia Wodzinska for getting me started in the lab and keeping me company in the cold basement. Finally I also owe gratitude to my supervisor Thomas Heimburg for patiently answering my many questions.

Resume

Det negativt ladede phospholipid dimyristoyl phosphatidylglycerol (DMPG) har ved pH over 6 og en ionstyrke under 100 mM, en mærkelig opførsel i faseovergangen fra gel til flydende lipider. Lipidet har en bred faseovergang med tre kalorimetriske peaks, der menes at være udtryk for en intermediær fase. Denne fase viser specielle fysiske egenskaber såsom øget viscositet og større gennemsigtighed. Der findes flere teorier for dens struktur, men endnu er der ikke opstillet nogen fyldestgørerende teorier der ikke kan modbevises.
Jeg har med viskometri og kalorimetri undersøgt pH afhængigheden af hhv. viskositeten og varmekapaciteten af DMPG opløsninger med lav ionstyrke som funktion af temperatur. Mine målinger viser at varmekapacitetsprofilerne ikke ændrer sig betydeligt for pH over 6, mens for pH under 6 ses der kun et peak i profilen som bevæger sig mod højere temperatur med faldende pH. Mine viskositetsmålinger viser at den intermediære fase tydeligvis har en højere viskositet end i gel og den flydende fase, særligt for $pH \geq 6$. Den maksimale viskositet vokser med pH indtil pH 8, og den intermediære fase kan tilsyneladende inddeles i to regioner, den første med meget høj viskositet, den anden med noget lavere relativ viskositet faldende mod ca. 1.1. Det ser ud til at denne inddeling cirka svarer til den inddeling af varmekapacitetsprofilen, der skabes af placeringen af de tre peaks.

The experiments were performed in the Membrane Biophysics Group from February 2008 to May 2008.

I have written two appendices, it should not be necessary for the understanding of my project to read these.

Contents

Chapter 1

Introduction and motivation

All living cells are surrounded by a membrane as well as many of their components such as mitochondria and the golgi apparatus. Therefore understanding the physics of membranes will contribute to the understanding of how cells work, or how life works. The negatively charged phospholipid dimyristoyl phosphatidylglycerol (DMPG) has been used as a model for for membranes to improve the understanding of negatively charged membranes. But it turns out that below physiological salt concentrations or more accurately at an ionic strength below 100 mM and a pH value above 6, DMPG shows a peculiar thermal behavior with a broad intermediate phase in the transition from gel to fluid lipids. This behavior can also be triggered in electrically neutral lipids by adding the negatively charged drug Losartan. The question is if this strange behavior has a biological relevance. The intermediate phase has an unknown structure different from the vesicular structure of the gel and fluid phases. Perhaps cells make use of a similar concept to trigger structural changes in their membranes. Triggering structural changes by changes in temperature, pH and salt concentration could potentially be used in targeted drug delivery, releasing encapsulated drugs. In particular if the theory of Riske et al., that the intermediate phase consists of perforated vesicles is correct.
The goal of this thesis is to examine the pH dependence of the phase transition of DMPG by using Differential Scanning Calorimetry and viscometry. The pH dependence of the viscosity has not been examined before. Determining the effects of varying pH could be relevant to see if the strange thermal behavior has a biological relevance, as it is known that pH can change locally in the cells in contrast to for example temperature.

Chapter 2

Theory

2.1 Membranes

All living cells are surrounded by a membrane. The function of the membrane is to be a selectively permeable border to the surroundings. Biological membranes consist of lipids and proteins. The proteins act as selective channels or are involved in cell signalling. The lipids are amphiphilic molecules, they have a hydrophilic headgroup and a hydrophobic tail consisting of hydrocarbon chains. When exposed to water the lipids therefore spontaneously form structures, in which the headgroups turn towards the water and the hydrocarbon chains turn towards each other. Examples of such structures are the lipid bilayer, micelles, inverse hexagonal phases etc. See figure 2.1. All biological membranes consist of lipid bilayers with a thickness of approximately 5 nm. Different cell membranes have different protein and lipid composition, the specific composition gives a specific function/ability.

The membrane is made of three classes of amphiphilic lipids: Phospholipids, glycolipids and steroids. The most abundant are the phospholipids. They can be divided into four subclasses: Diacyl-Phosphatidylcholine (PC), Diacyl-Phosphatidylethanoalimine (PE), Diacyl-Phosphatidylglycerole (PG) and Diacyl-Phosphatidylserine (PS). The latter two lipids are charged. The charge comes from the negatively charged phosphate group. The fraction of negatively charged lipids in a membrane is typically 10-20 %, it can however be up to 40 % in mitochondria. The rest of the lipids are either zwitterionic (the charges in the lipid neutralize each other) or neutral. Positively charged lipids normally do not occur.

I have been working with a lipid called DMPG. DMPG is an abbreviation of 1,2 Dimyristoyl-sn-Glycero-3-[Phospho-rac-(1-glycerol)], it belongs to the class of phospholipids called

Figure 2.1: *Different lipid structures. From the left: Micelle, bilayer and inverse hexagonal phase. [15]*

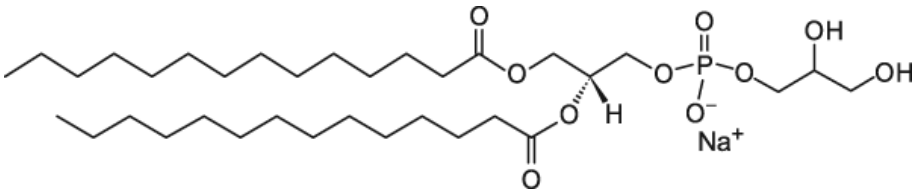

Figure 2.2: *The chemical structure of the sodium salt of DMPG.*

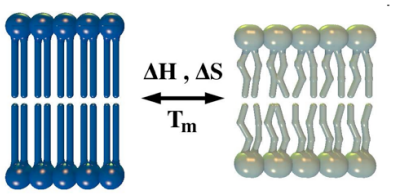

Figure 2.3: *The lipid phase transition from gel to fluid phase. When the lipids melt the enthalpy and the entropy increases.* T_m *is the transition temperature.*
[16]

Diacyl-Phosphatidylglycerole because of the glycerol group. It has two hydrocarbon chains with 14 carbons each. DMPG has one negative charge from the phosphate group. See figure 2.2 for chemical composition.

2.1.1 Phases and Phase Transitions

The lipid molecules can arrange themselves with different kinds and degrees of order. This corresponds to different phases. There are two main lipid phases: A highly ordered gel phase and a disordered fluid phase. See figure 2.3.

If the hydrocarbon chains are saturated (as they are in DMPG), rotations around all the C-C bonds are possible. When none of the C-C bonds are rotated (called an all-trans configuration) the lipids have minimal internal energy. The hydrocarbon chains are parallel and fully extended. This phase is called the crystalline gel phase. There is only one possible configuration that is all-trans so this configuration has minimal entropy, because $S = k_B \ln g$ where g is the number of accessible states and k_B the boltzmann factor. When the temperature is increased the number of accessible states/the entropy also increases. This is due to rotations in the C-C bonds and is called chain-melting. The rotations make the hydrocarbon chains kinky and hence leads to a higher area and smaller thickness of the fluid than of the gel phase where the chains are more straight. The area difference is about 25 %. See figure 2.3.

There also exists different subclasses of gel and lipid phases. In figure 2.4 you see some examples of different gel and fluid lipid bilayer phases. As mentioned above the entropy increases in the transition from gel to fluid. This is caused by a heat uptake as we have the connection $dS = \frac{dQ}{T}$. So by measuring the heat uptake of the lipids as a function of

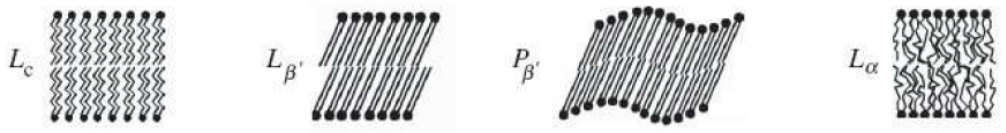

Figure 2.4: *Different lipid phases. From the left: crystalline, gel, ripple and fluid phases.*

temperature, we can tell if there is a phase transition. A very sharp peak in the heat capacity profile corresponds to a phase transition. Thus measuring the heat capacity profile is a common technique to determine phase transitions. Lipids do not melt independently of each other, they melt in cooperative units. The bigger the units are, the sharper peak we get in the heat capacity profile.
A more precise definition of a phase transition is a first order transition where the enthalpy makes a sudden change at a well-defined temperature, therefore the heat capacity $C_p = dH/dT$ is infinite and the proces infinitely slow. But in the real measurements we cannot scan infinitely slow and the heat capacity is typically not infinite.

Lipid phases do not only vary in the conformation of the single lipid, but also in the overall geometry of the aggregation of lipids. See figure 2.1 for examples.

2.1.2 Transition Temperature

The transition temperature of a phase transition can be defined as the temperature at which 50 % of the lipids are in the first phase and 50 % are in the second phase. So the likelihood to be in the two phases is the same. The transition temperature can be calculated from the difference in enthalpy and entropy of the two phases:

$$\frac{P_2(T_m)}{P_1(T_m)} = K(T_m) = \exp\left(-\frac{\Delta H - T_m \Delta S}{kT}\right) = 1 \iff \Delta H - T_m \Delta S = 0 \iff T_m = \frac{\Delta H}{\Delta S} \tag{2.1}$$

2.2 Membrane Electrostatics

About $10 - 40\%$ of all naturally occuring lipids are charged. They usually have one or two negative charges. The charged lipids give rise to a surface charge density σ and therefore also an electrical potential of the membrane.
By assuming that the membrane surface is a plane surface with a uniform charge density and by considering the charges as point charges, one can derive a simple formula for the membrane potential. This simplified membrane model is called the Gouy-Chapman model. A derivation of the formula is given in appendix B. The membrane potential can be approximated for univalent ions to:

- high surface potentials ($e\Psi_0 \gg 2kT$):

$$\Psi_0 = \frac{2kT}{e} \ln\left(\sigma\sqrt{\frac{1}{2\epsilon\epsilon_0 c_0 kT}}\right) \tag{2.2}$$

for $\sigma > 0$

$$\Psi_0 = \frac{2kT}{e} \ln\left(-\sigma\sqrt{\frac{1}{2\epsilon\epsilon_0 c_0 kT}}\right) \tag{2.3}$$

for $\sigma < 0$

- low surface potentials ($e\Psi_0 \ll 2kT$):

$$\Psi_0 = \frac{\sigma}{\epsilon_0 \epsilon \kappa} \tag{2.4}$$

Ψ_0 is the potential at the membrane surface.

c_0 is called the ionic strength of the solution. It is defined as:

$$c_0 = \frac{1}{2}\sum_i z_i^2 c_{i,0} \tag{2.5}$$

- with i being the different kinds of ions in the solution. z is the number of charges per ion and $c_{i,0}$ is the concentration at infinite distance from the membrane. σ is the surface charge density.
ϵ and ϵ_0 is the relative and the vacuum permitivity respectively.
κ is defined by $\kappa^2 = \frac{2e^2 c_0}{\epsilon\epsilon_0 kT}$

The limit of the high potential region depends on the surface charge density. For a 100 % charged membrane at an ionic strength below 100 mM, the high potential approximation is always valid. According to Träuble et al.[1] the high potential approximation is fully valid down to a 20 % charged membrane if the ionic strength is around 10-20 mM. Therefore the membrane potential of my samples can be approximated with the high potential approximation except for the very low pH samples (at least below 4 where I later show that approx. 50% of the lipids are charged).

2.2.1 Shifts in T_{trans}

The fluid state occupies an area that is approximately 25 % larger than the area of the gel state. As the coulomb forces decrease with distance, this means that the electrostatic interactions between the charged groups are larger in the gel state. Thus a decrease in the number of net charged head groups will increase the stability of the gel state more than that of the fluid state. Lowering the surface charge therefore shifts the phase transition to higher temperatures.[2] This can be done by adding ions to the solution. Träuble et al.

[1] Träuble et al. 1976.
[2] Träuble et al. 1976

have derived a formula for the shift in transition temperature by using the Gouy-Chapman theory, and making the assumption that the change in electrostatic free energy when going from the gel to the fluid state, is purely a result of the expansion of the membrane at constant charge per polar group:

$$\Delta T_t = \frac{-2kT}{e}\frac{L}{\Delta S^*}\sigma\Delta f + \frac{\epsilon}{\pi}\left(\frac{kT}{e}\right)^2\frac{L}{\Delta S^*}\kappa\Delta f \tag{2.6}$$

Where Δf is the increase in molecular area at the gel to fluid transition.
σ is the surface charge density.
ΔS^* is the difference in entropy of the gel and fluid state of the uncharged membrane.
ϵ is the dielectric constant.
L is Avogadro´s number.
k is the boltzmann factor and
e is the elementary charge.

Thus the shift in transition temperature is linearly related to the surface charge density in this simplified model.

2.3 DMPG and its Mysterious Phase Transition

Due to the presence of acidic headgroups, most cell membranes have a net negative surface charge. In prokaryotes the most abundant anionic phospholipid headgroup is phosphatidylglycerol (PG). PG-lipids have therefore been widely used as a model for negatively charged membranes. DMPG is a lipid with a phosphatidylglycerol headgroup and two carbon chains with 14 carbons each. It has been considered a suitable lipid for membrane modelling because under physiological conditions it shows a gel-fluid transition at the convenient temperature of 23°C. In solutions of more than 100 mM NaCl DMPG shows a heat capacity profile similar to the zwitterionic lipid dimyristoyl phosphatidylcholine (DMPC) with a sharp peak at 23° C. The resemblence is due to the fact that the two lipids have identical carbon chains. Only the head groups differ. But at an ionic strength below 100 mM NaCl, DMPG has been found to have a complex thermal behaviour. It shows a wide gel-fluid transition regime with at least two peaks, ranging from around 18 to 35°C, depending on salt concentration. The first peak is very sharp. Below and above the transition regime, that is in the gel and fluid state, the lipids form vesicles. See figure 2.5. The structure of the intermediate phase is unkown.

This peculiar behaviour was first studied by Salonen et al. in 1989. They interpreted the first peak in the DSC trace as a main gel-fluid transition and the second peak as a not well characterized post-transition. Their studies were followed by Heimburg and Biltonen in 1994, who suggested that the region between the two main peaks represented a gel-fluid transition region. They measured a sharp decrease in the light scattering at the first transition peak followed by a sharp increase at the last peak for low ionic strength dispersions of DMPG. Furthermore their viscosity measurements of lipid dispersions showed the same correlation with the DSC profile: A high viscosity in the temperature range between the two outer C_p peaks. Heimburg et al. thus suggested that the intermediate phase consisted of a three-dimensional bilayer network. Since then the intermediate phase of DMPG has been studied extensively, but the exact nature of it remains unknown. Here is a summary of the measured properties of DMPG at low ionic strength and a pH above 6.

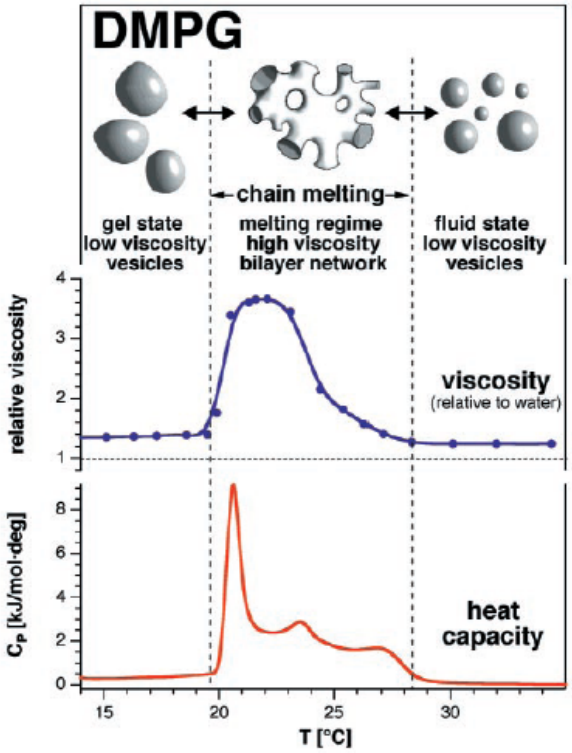

Figure 2.5: *The phasetransition of DMPG. The assumption that the structure of the intermediate phase is a bilayer network (sponge phase) has not been proved. From Heimburg et al., Network formation of lipid membranes, 1999.*

Below the First Transition Peak, the Gel State

Depending on the ionic strength and pH of the solution, the first transition peak is situated approximately at 18° C. The lipids form bilayer vesicles. The vesicles scatter light and the dispersion thus looks a little milky. The dispersion shows low viscosity.

Above the Last Transition Peak, the Fluid State

Again depending on pH and ionic strength the last peak is located at app. 35° C. The lipids form vesicles, but they are now smaller than below the transition regime. The viscosity of the dispersion is low and it looks milky.

The Transition regime

The intermediate phase shows a higher viscosity, conductivity and transparancy than the gel and fluid phases. A sample with a temperature within the intermediate region looks transparent. Furthermore Riske and Lamy-Freund have measured an increase in the electrostatic surface potential.
As mentioned above, DMPG at an ionic strength of 100 mM shows a DSC profile very similar to that of DMPC - it has a single sharp peak. The melting enthalpy of the DMPG peak has been measured by Riske et al.[3] to be 5.7 ± 0.8 kcal/mol and for DMPC (at $c_0 = 6$ mM) $\Delta H = 5.0 \pm 0.8$ kcal/mol. Riske et al. also measured and integrated the broad transition regime of DMPG at low ionic strength for temperatures above 15° C and got an enthalphy value of $\Delta H = 5.2 \pm 0.8$ kcal/mol. The fact that the transition enthalpy of the broad transition regime is approximately the same as for the sharp melting transition, suggests that at low ionic strength the chain melting is spread over a large temperature range. This theory is supported by the measurement by Riske et al. of a continuous decrease in membrane packing and bilayer thickness with temperature within the transition region.
Schneider et al.[4] investigated the phasetransition of PG lipids with different chainlengths and showed that for increasing chainlength the transition regime narrows, PG lipids that have a chainlenght of 16 carbon atoms show only one heat capacity peak, whereas a length of 13 carbon atoms give a wider transition.

Different Theories for the Structure of the Intermediate Phase

Heimburg et al. suggested in 1999 that the intermediate phase of DMPG consists of a three dimensional extended bilayer network, a socalled sponge phase, see figure 2.5. This was supposed to explain the increase in viscosity and the decrease in sample turbidity. The likelihood of this theory has later been examined by Riske et al. and Kinnunen et al. Kinnunen et al. (2007) heated up labeled DMPG vesicles letting the vesicles pass through both the upper and lower boundaries of the intermediate phase, and still even after passing the boundary temperatures up to 24 times (by heating/cooling) the labels where retained within the initial vesicles. Thus there cannot be much mixing of the lipids

[3] Riske et al. 2002
[4] Schneider et al. 1999

in the intermediate phase. If the intermediate phase was a bilayer network, fusion of vesicles would be required in the transition from the vesicular states of the gel and fluid phases to the intermediate phase, and there should therefore be mixing of the lipids. Therefore Kinnunen et al. concluded that no vesicle fusion happens within the intermediate phase and that the sponge phase theory is unlikely. Similarly Riske et al. showed a lack of vesicle fusion.

Riske et al. (1997) have come up with another hypothesis: That the vesicles aggregate above and below the intermediate state, but not in the intermediate state itself. They suggested that the decrease in light scattering and increase in viscosity (because of increased repulsion between vesicles) in the intermediate phase is due to disaggregation of vesicles. The strength of this theory has also been tested by Kinnunen et al. (2007). They measured particle sizes above and below the intermediate region, that are close to the vesicle sizes seen in cryo-TEM images of Schneider et al. and also with resonance energy transfer experiments, they showed that formation of aggregates in the gel and fluid phase is unlikely. Furthermore Kinnunen et al. have done some approximate calculations to test if the increase in viscosity could be caused by repulsion between vesicles. Their conclusion is that this might be the case, but for the intermediate phase they used a relative viscosity of 3.6 for 45 mM DMPG from Schneider et al. in their calculations. This value is much too low if you compare with my viscosity measurements that gave a relative viscosity of up to more than 20 for a concentration of just 2 mM. They may have used too high a scan rate in the viscosity measurement.

A more recent hypothesis from Riske et al. (2004) is that the intermediate phase consists of unilamellar vesicles with perforations. They believe to have shown with x-ray scattering that the intermediate phase cannot consist of multilamellar vesicles or a sponge phase, but disrupted unilamellar bilayer vesicles with pores. This is supposed to exlain the increase in electrical conductivity and the decrease in turbidity as the light has passage through the holes. The theory is also supported by experiments with giant DMPG vesicles grown by electroformation. When cooling the vesicles below the offset of the intermediate phase (and thus entering it), the vesicles dissappear, but reappear when the the temperature is again increased above the upper intermediate phase boundary. But if the sample is kept within the intermediate phase region for more than 15 min, the giant vesicles though dissappear and only small vesicles are observed. With this experiment Riske et al. believe to have shown that the vesicle structure is preserved in the intermediate phase, since giant vesicles are not spontaneously formed by changes in temperature, also the dissappearance of the vesicles can support the pore theory.
This theory is also found likely by Kinnunen et al.[5] and seems to be the most realistic theory presented sofar. But the origin of the transformation into tattered vesicles is still unexplained, and whether single vesicles can explain the increase in viscosity is questionable. So even after almost 20 years of research a full and bulletproof description of the structure of the intermediate phase of DMPG has still not been seen.

Ionic Strength Dependence

The thermal behaviour of charged lipids depends on the concentration of other ions in the solution, because the ions affect the membrane potential by shielding and/or binding

[5] Kinnunen et al. 2007

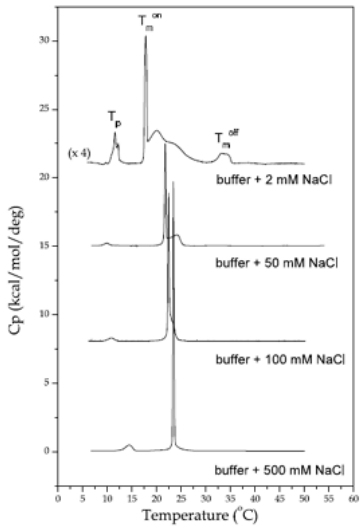

Figure 2.6: *DSC traces obtained with 10 mM DMPG in buffer (10 mM Hepes pH 7.4) and different NaCl concentrations. For better visualization, the scans were shifted from $C_p = 0$ (adapted from Riske et al., 2002).*

to the charges of the membrane. And changing the membrane potential also affects the thermodynamic variables, as we for instance have that:

$$dH = TdS + Vdp + \pi dA + \Psi dq + \dots \tag{2.7}$$

Where Ψ is the membrane potential.
As the ionic strength increases the transition region narrows until it the two main peaks collaps into one at app. $c_0 = 100$ mM and a temperature of 23° C. See figure 2.6. If the ionic strength is further increased the transition temperature rises to 29°C at 2 M NaCl[6].

pH Dependence

One could argue that the hydrogen ions just contribute to the ionic strength of the solution. But they are normally not taken into account when calculating the ionic strength because protons bind much more strongly to the phosphate groups of the lipids than larger ions as for example Na^+. The H^+-PG^- association constant is assumed to be app. 15.8 M^{-1} [7] and the association constant for $Na^+ - PG^-$ varies in the literature from 0.1 to 1 M^{-1}. [8] Furthermore the concentration of protons in the solution is normally much lower than the salt concentration, therefore the effect of binding is more important than shielding for protons, contrary to sodium ions. So one has to look at the effects of the two kinds of ions seperately.
But decreasing pH should have approximately the same kind of effect as increasing ionic strength, perhaps just on a different scale. Riske et al. have measured that for low pH the transition is sharp and for a pH above 6 the DSC profile is independent of medium pH, which suggests that above pH 6 the phosphate groups are fully deprotonated[9].

[6] Riske et al. 2001
[7] Riske et al. 1997
[8] Riske et al. 1997
[9] Riske et al. 2002

The disappearance of the broad phase transition at high ionic strength and low pH indicates that the intermediate phase is related to the presence of charged head groups or high surface potential. Another indication of this is the fact that complexes of the negatively charged compound Losartan with vesicles of the zwitterionic lipid dimyristoyl phosphatidylcholine, show a behavior similar to that of DMPG at low ionic strength.[10]

Concentration Dependence

In general the broadness of the phase transition decreases with increasing DMPG concentration. But below a lipid concentration of $c = 0.4 \pm 0.2$ mM the peculiar phase transition has been reported to disappear and be replaced by a single sharp peak.[11]

[10] Scneider et al. 1999
[11] Riske et al. 2002

Chapter 3

Materials and Methods

3.1 Preparation of Samples

The solutions made for the DMPG samples used in calorimetric and viscosity measurements all contained 10 mM NaCl and 1 mM EDTA. They were prepared by weighing off the necessary amounts with an uncertainty of $\pm$0,0001 g and dissolving this in a known volume of milipore water. These amounts were calculated with the relations

$$c = \frac{n}{V} \text{ and } n = \frac{m}{M} \tag{3.1}$$

EDTA is a strong Ca^{2+} binder and is added both to prevent interactions between the membranes and calcium ions which are especially strong for charged lipids like DMPG and to prevent the sample from being eaten by bacteria. To make sure that pH was kept constant in the respective samples, different buffers with a pK_a of $\pm$1 of the desired pH value was used. The buffer concentration was in all cases 5 mM. Beneath is a list of the used buffers.

Desired pH	Used buffer	pKa of used buffer at 25°C
3	Citric acid ($C_6H_8O_7 \cdot H_2O$)	3.15
4	Citric acid	4.77
5	Citric acid	4.77
6	MES ($C_6H_13NO_4S \cdot xH_20$)	6.15
7	Hepes ($C_8H_12N_2O_4S$)	7.48
8	Hepes	7.48
9	TAPS ($C_7H_17NO_6S$)	8.43
10	Sodium bicarbonate ($NaHCO_3$)	10.32
11	Sodium bicarbonate	10.32

To adjust the pH small amounts of NaOH or HCl was added. After preparation the buffers were kept in a fridge. Adding NaOH or HCl changes the ionic strength of the buffer. As I noted the added amounts of acid or base I can calculate the change in ionic strength. See table beneath.

For the DMPG samples the sodium salt of DMPG purchased from Avanti Polar Lipids was used. To make the DMPG solution for measurements the DMPG container was first taken out of the freezer and heated up to room temperature. This is important before opening the container to avoid that the lipids bind water. Then enough DMPG was weighed off to make app. 4 mL solution with a concentration of 2 mM. Calculated amount of buffer was added. To dissolve the lipid the glass bottle (closed with a lid) was heated up under the water tap and vortexed repeatedly.
In the table beneath I calculated the total ionic strength of each DMPG sample. The contributions are: 1 mM from EDTA, 10 mM NaCl, 1 mM from the sodium ions from the DMPG powder, varying ionic strength contributions from the pH adjustment and finally 5 mM from the buffer if the used buffer is the salt of an acid (is the case for pH 10 and 11) and 2.5 mM if the acid powder was not a salt (is the case for all other pH). I don´t

	pH 4	pH 5	pH 6	pH 7	pH 8	pH 9
c_0 from pH adjustment	3.0 mM	4.6 mM	2.8 mM	1.0 mM	2.5 mM	2.8 mM
Total c_0	17.5 mM	19.1 mM	17.3 mM	15.5 mM	17 mM	17.3 mM

have the values for pH 3, 10 and 11, but for pH 10 and 11 the ionic strength without the pH adjustment contribution is 17 mM. So the ionic strength of these two samples must lie around 20 mM.
Thus the ionic strength of my samples varies from 15.5 to around 20 mM, this gives a variation in ionic strength of 30 %. But the membrane potential in the high potential regime is proportional to $\ln(1/\sqrt{c_0})$, so this only gives a variation in membrane potential of 6 %.

3.2 Differential Scanning Calorimetry

For my measurements of the heat capacity profiles I used a VP-DSC, produced by Microcal (Northhampton/MA, USA). The Differential Scanning Calorimetry is widely used to obtain thermodynamic properties of lipid membranes as the heat capacity profile can be used to find several properties like transition temperatures and melting entalpy. It consists of two cells enclosed in an adiabatic box, with no heat transfer to the surroundings. One cell is for the sample, the other for a reference solution. The pressure in the cells is approximately 50 psi = 4.4 bar when the lid is properly tightened. During the scan the temperature is either increased or decreased with a defined scan rate and the power added to the respective cells is adjusted so the two cells have the same temperature. The difference in the power needed to heat the two cells is called the excess power ΔP. The excess heat added to the sample can be found by integrating under the assumption that Δt is small enough for ΔP to be constant during this time period:

$$\Delta Q = \int_t^{t+\Delta t} \Delta P(t')dt' \simeq \Delta P \cdot \Delta t \tag{3.2}$$

The heat capacity at constant pressure is given by the heat required to increase the sample temperature by ΔT at constant pressure. The excess heat capacity is given by the excess heat, it follows from eq. 3.2:

$$\Delta C_p = \frac{\partial Q}{\partial T} \simeq \frac{\Delta Q}{\Delta T} \simeq \frac{\Delta P}{\frac{\Delta T}{\Delta t}} \tag{3.3}$$

Where $\frac{\Delta T}{\Delta t}$ is the scan rate.

3.2.1 Handling the Heat Capacity profile

The heat capacity at constant pressure is equal to:

$$c_p = \left(\frac{dQ}{dT}\right)_p = \left(\frac{dH}{dT}\right)_p \tag{3.4}$$

Because we have the relation $dH = dE + d(pV) = TdS + Vdp = dQ$ when $dp = 0$. We can therefore get the entalpy by integrating the heat capacity curve:

$$\Delta H = \int_{T_1}^{T_2} c_p dT \tag{3.5}$$

There is a contribution to the enthalpy called the intrinsic enthalpy that has nothing to do with the phase transition, because the lipid also has a heat capacity different from zero outside of the melting transition. We want the data to say something about the heat uptake of the transition itself. Therefore we subtract this contribution to the heat capacity by deleting the phase transitions from the curve, fitting the rest of the curve to a polynomial and subtracting this from the original heat capacity profile. This is called subtracting the baseline.

The enthalpies of the peaks, the peak temperatures and the upper and lower limits of the melting regime were found by using the computer program Igor and a macro made by Kaare Græsbøll and Andreas Blicher. By the limits of the melting regime I mean the temperature where the broad transition regime or the two outer peaks in the transition regime fade out. It is difficult to define exactly where this is, so determining these temperatures is associated with some uncertainty. But this is how I determined them:
The macro was programmed to find the upper melting temperature by drawing the tangent of the peak from 80 to 50 % of the peak. The macro could not find the lower melting temperature, so I found this by zooming in on the lower peak and drawing a suitable tangent to the peak. I used the cursor to find two points on the tangent and calculated the intersection of this straight line with the T-axis.

3.3 Viscosity Measurements

Viscosity is a measure of a fluids thickness or resistence to flow. The thicker the fluid the higher viscosity. Or more accurately it is a measure of a fluids resistance to being deformed by shear stress.

The viscosity was measured with a rotation viscometer of the model Low Shear 30 Sinus from the firm Contraves, Switzerland. The rotation viscometer works as follows: A small metal cup filled with the sample is rotated with a constant velocity. A small pendulum is hanging down into the cup so that the weight is covered by the sample. It is important that the pendulum is exactly centered in the cup to prevent large fluctuations in the viscosity because of variations in pendulum to wall distances. This was regulated by adjusting the two screws underneath the apparatus. At constant rotation velocity and temperature the measurements varied 0.2-0.4. The zero point of the apparatus was adjusted by turning the upper screw, while the engine was turned off, until the machine displayed 0.

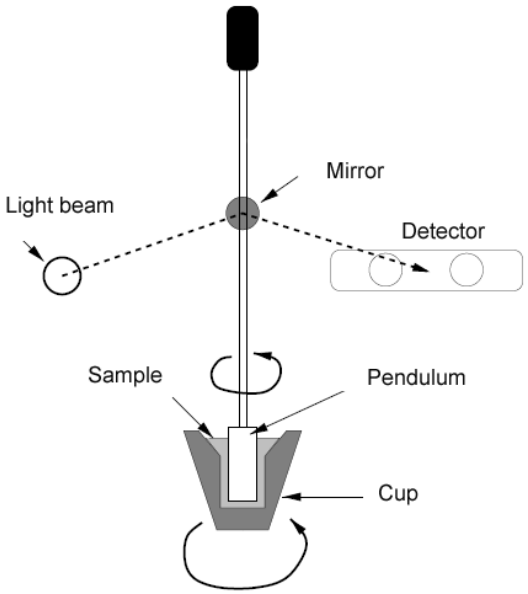

Figure 3.1: *Simplified drawing of the viscometer. Copied from the thesis of Peter Grabitz 2001.*

Figure 3.1 shows the principle behind the viscometer. A light beam is reflected in a mirror attached to the pendulum, to two photodetectors. The rotation viscometer utilizes the fact that torque is required to rotate an object in a fluid. In this case an electronic device exerts just enough opposite torque on the pendulum so the photodetectors measure a light intensity equal to the light intensity measured when the cup is not rotating. The voltage required to exert this torque is the value displayed by the machine - as a measure proportional to the viscosity.
The temperature of the sample is regulated by sending water from a large water tank under the metal cup and concealing the apparatus with a plexiglas cage and a flamingo cage. Temperature measurements are done by a thermometer situated underneath the sample cup. To prevent the sample from drying out there is a water-filled container inside.

3.4 Fluorescence Microscopy

The structure of the intermediate phase of DMPG is still unknown. There has been taken some Electron Microscopy pictures of the three phases but in order to take such pictures, the samples have to be frozen down and this might affect the structure. Therefore it would be relevant to try to take pictures with a fluorescence microscope, where the lipid is not frozen down or attached to anything but moves freely in the solution and we can freely vary the temperature.

3.4.1 Preparation of the Sample

Make a methanol/dichloromethane solution of DMPG. 4 mg of DMPG is weighed off into a 4 ml glass. A glass pipette is used to add 4 ml of solvent. The solvent is a methanol/dichloromethane mixture with a volume ratio of 1:2.

Add label. The used fluorescence label is DiI. From the 4 ml solution 200 μl are transferred to a new glass. Enough DiI (dissolved in the same solvent) is added to make $n_{DMPG} : n_{DiI} = 500 : 1$

Removal of solvent. A petriplate with water is put on a heater set up inside the fume board and the sample is put in the water bath. An air tube is set up so it is blowing down air very softly on the sample. Heating is continued until the sample is completely dried out.

Transfer sample to plates. To reduce the surface tension of the solution so it spreads out more on the plate, 200 μl trifluoroethanol (TFE) is now added. A drop of 6 μl is put on a cleaned plate. This final sample is dried out in a dessicator for at least three hours.

3.4.2 Setting up the Microscope

The sample plate is attached to one side of a small plastic frame with a thin layer of grease. The plastic frame is then screwed onto a brass plate. The metal plate is hollow and attached to a water pump pumping water from a large temperature regulated water tank. See figure 3.2. Finally the buffer is added into the plastic frame and a small glass plate is put on top. This device is then put under the microscope. The microscope is lit up by a mercury lamp and the pictures are taken by a CCD camera with the use of the computer program Maxim.

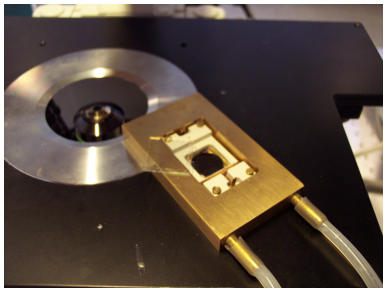

Figure 3.2: *The microscopy sample.*

Chapter 4

Results

4.1 The Heat Capacity Profiles

When you record a profile you normally record 3 scans, 2 upscans (increasing temperature) and one downscan (decreasing temperature) or one down and two upscans. The DSC peaks are shifted a little to lower temperatures for the downscans compared to the upscans. This is called hysteresis.
For all other pH values than pH 4 and 10 I chose one of the upscans to represent the measurement. But for the two mentioned pH values the upscans were not nice enough, so I had to choose the downscans instead. For pH 10 I then added the hysteresis measured as the difference in the temperature of the big sharp peak between up and downscan (0.181°) to all the measured temperatures. But this could not be done with the pH 4 curves because there was a big difference in the overall shape of the three curves and the two upscans had a difference in peak temperature of more than three degrees.
The reason why you do a second scan (where the temperature changes in the opposite direction to the first one) is to check if the process is reversible. The reason for the third scan is to check if the data are reproducible. For pH above 6 the three curves where close to identical. But for pH 6 and below there was a lack of reversibility and reproducibility. It was not critical for pH 6, here I got a nice curve doing the first upscan, the two next curves looked different but a little similar. It got worse for pH 5, 4 and 3, here the three scans looked very different, and some of them had a lot of extra small peaks.
I subtracted the baseline of the DSC scans, the resulting heat capacity profiles are seen in figure 4.1. For $pH \geq 6$ I used a scan rate of 5°/h for lower pH I used 10°/h.

The curve for pH 3 has a slightly negative heat capacity just before the large peak, this cannot be true and is due to a wrong subtraction of the baseline. But it can only be avoided if you assume, that some of the curve before the large peak is also a part of the transition, so you must subtract it from the baseline. But noone knows if this is correct, so I did not make the assumption, but just showed the curve I get when I subtract the baseline as I normally would have done.

The scans can be divided into two groups:

- For $pH \geq 6$ the heat capacity profile shows the characteristic broad transition with three peaks. The first one is always very sharp, then there is one little broad peak

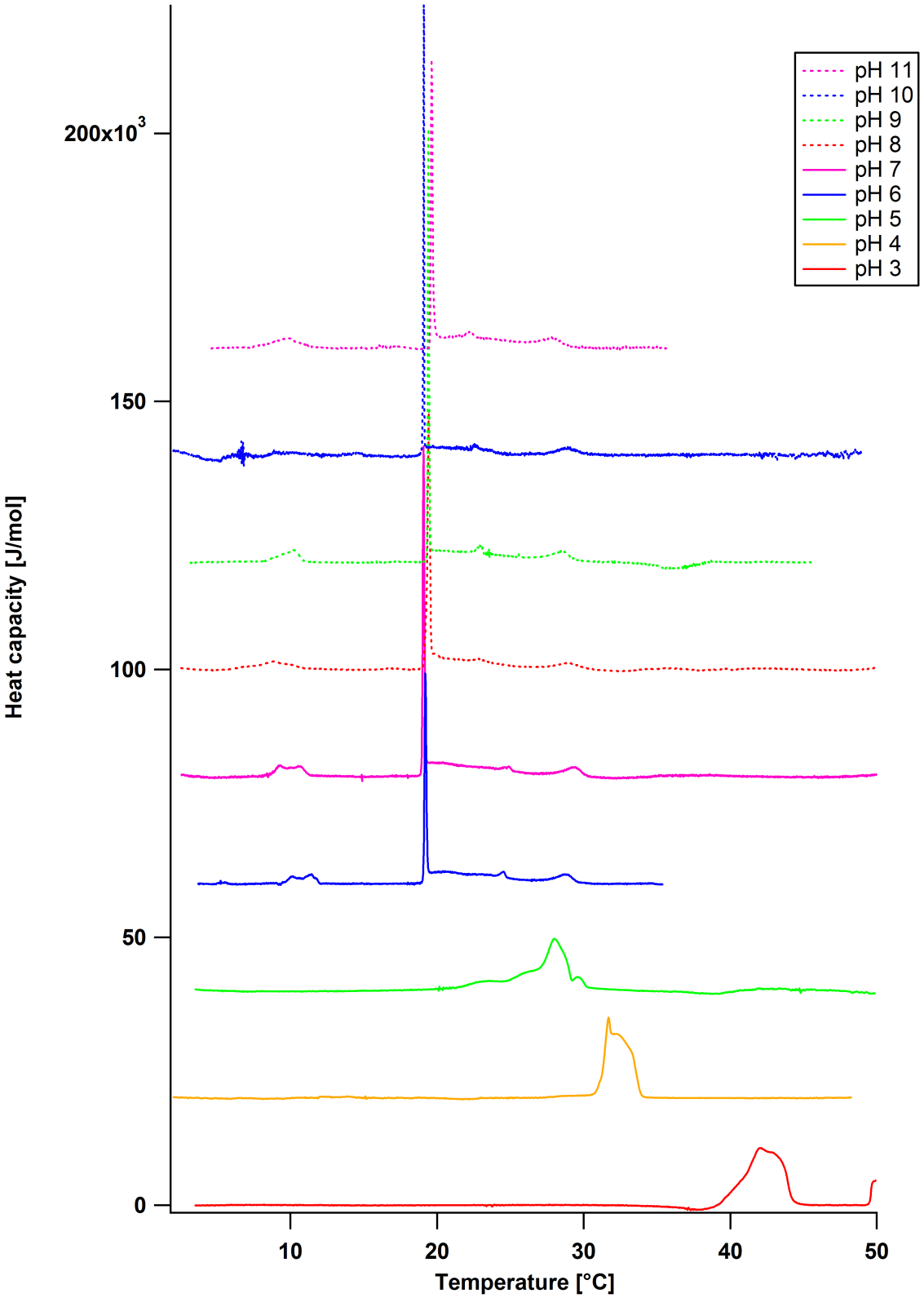

Figure 4.1: *Heat capacity curves for different pH. All samples contain 2 mM DMPG and 10 mM NaCl. The curves are plotted with different offsets.*

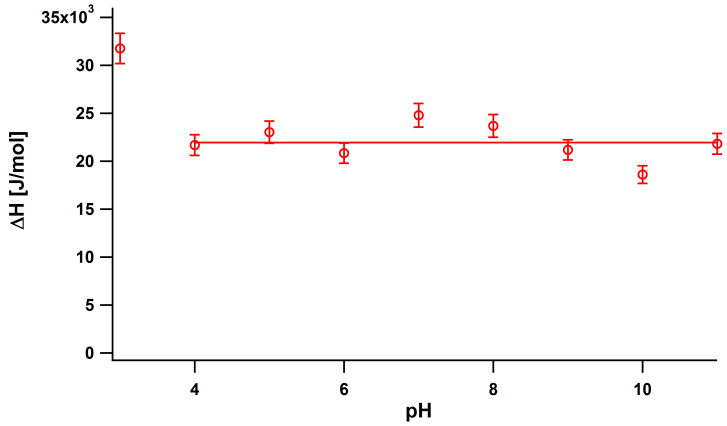

Figure 4.2: *Values for ΔH for different pH averaged over scans for the same sample.*

somewhere in the middle of the regime and the melting regime is ended by another small broad peak. This corresponds nicely to what has been measured by others.[1] Furthermore the lipid has a pretransition around 9-10°C that sometimes consists of two small peaks.

- For pH 5 to 3 there is only one peak. This is not the entire truth though, because the two other scans out of the three sometimes had more smaller peaks, but there was always one obvious main peak which was quite broad. None of the scans looked like the scans in the other group.

I used the program Igor to integrate the C_p curves after subtracting the baseline and thereby got 2-3 ΔH values per pH depending on how many of the scans were useful. For each pH value I calculated the average ΔH, they can be seen in figure 4.2.

It is sometimes difficult to determine the baseline correctly, especially when the transition is broad as in this case. When the baseline is not determined perfectly the area under the curve is wrong, and the baseline on both sides of the peak is perhaps not zero as it should be. Therefore the integration depends very much on where you place the upper and lower boundary cursors. I saw cases where a slightly different cursor position changed the enthalpy by up to 1 kJ. In total I saw variations in the enthalpy for the same sample of up to 10 %. This is shown by error bars ($\pm$ 5%) in my graph. Besides that I also have uncertainties in connection with preparation of the sample.

Figure 4.2 shows that the enthalpy of the transition is close to constant for all pH except pH 3. Fitting all points except the point for pH 3 with a horisontal line gives an enthalpy of 21951 $\pm$ 673 J/mol.

I found the lower melting boundary $T_{lowermelt}$ - the temperature where the broad melting transition begins, the upper boundary of the melting transition $T_{uppermelt}$ and the temperature of the largest peak in the scan $T_{mainpeak}$. See the Materials and Methods section for details. The temperatures are plotted in figure 4.3. For pH 6 and higher $T_{mainpeak}$ is almost equal to $T_{lowermelt}$ because the main peak is the first peak in the regime and it is very sharp.

[1] Schneider et al. 1999, Riske and Lamy-Freund 2002 and 2001.

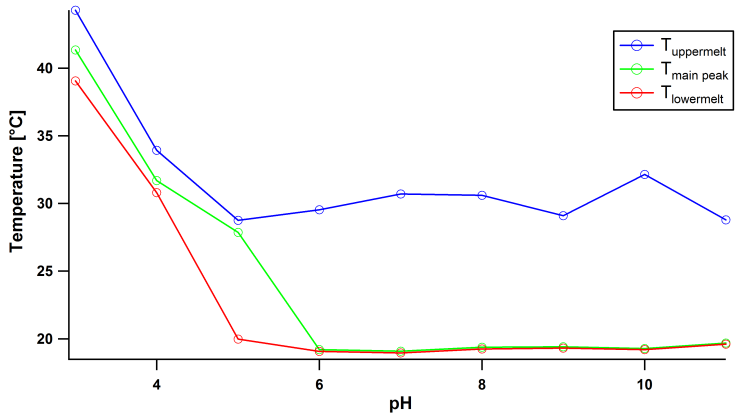

Figure 4.3: *Melting regime boundaries and peak temperatures from the DSC profiles as a function of pH.*

The graph shows that the temperatures are close to constant for $pH \geq 6$, but below pH 6 they increase rapidly.

4.2 Viscometry

4.2.1 Calculating the relative viscosity

The viscometer does not display the real viscosity, but a number proportional to the viscosity. To calculate the absolute viscosity you have to do calculations using the rotation velocity of the pendulum, the size of the pendulum etc. It is much easier to find the viscosity relative to another measurement with the same parameters so the unknown proportionality constants disappear. I did a measurement for a pure buffer with the same parameters as my other measurements (pendulum size and rotation velocity) and fitted the curve to a 3rd degree polynomial. See figure 4.4. The found polynomial was:

$$\eta(T) = K_0 - K_1 \cdot T + K_2 \cdot T^2 + K_3 \cdot T^3 \tag{4.1}$$
$$K_0 = 13.271 \pm 0.0801$$
$$K_1 = -0.41572 \pm 0.00958$$
$$K_2 = 0.0073695 \pm 0.000347$$
$$K_3 = -5.4939e-05 \pm 3.86e-06$$

The displayed values are the coefficient values $\pm$ one standard deviation.

To calculate the relative viscosity of the different samples I then used the polynomial to find the "viscosity" of the buffer at the exact temperatures that had been measured in the specific sample measurement. Then I divided each data point of the sample measurement by the calculated buffer "viscosities" at the same temperatures.

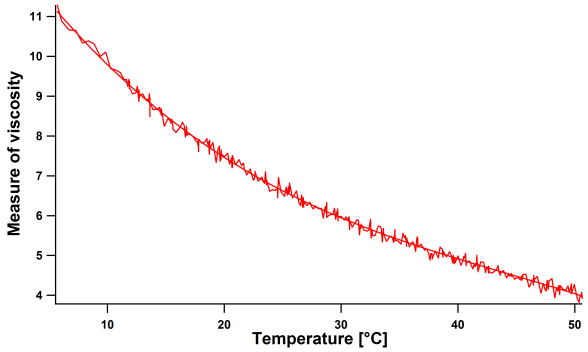

Figure 4.4: *Viscosity measurement of pure 5 mM MES buffer pH 6 with 10 mM NaCl plus fitted 3rd degree polynomial.*

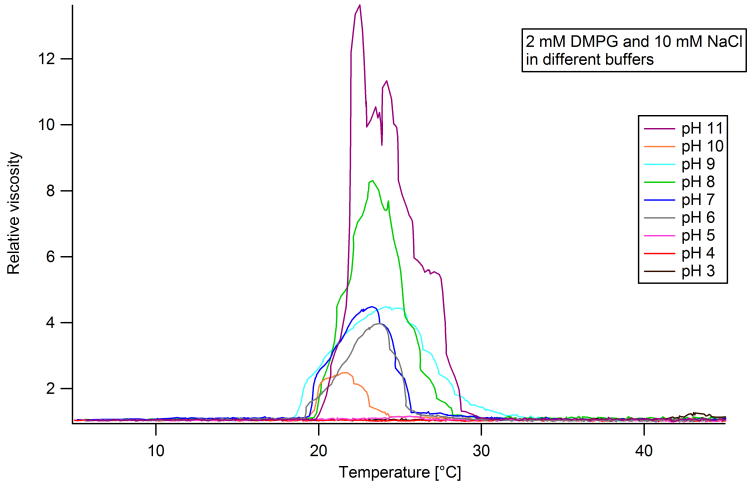

Figure 4.5: *The first viscosity measurements.*

4.2.2 Adjusting parameters

Measuring the viscosity should be a quite simple procedure. But it turned out to be less simple than I expected.

In figure 4.5 you see the first viscosity measurements I made. If you look closely you see that the curves have small arches for every step of one degree on the temperature axis. Before you start the viscometer you choose how much the apparatus changes the temperature at a time and for how long it is kept constant. Here I used the standard parameters which are 1° steps and the temperature is kept constant for 2 minutes, which corresponds to a scan rate of 30 degrees per hour. This is the reason for the arches on the graphs. When the temperature is changed by one degree it happens too fast for the sample to equilibrate, so the data points during this process do not follow the rest of the curve. Furthermore you see that there is no obvious connection between pH and viscosity. I thus decided to do the measurements again but with a lower scan rate. First I tried with 0.2° steps kept constant for 1 minute corresponding to a scan rate of 12 degrees per hour. This made the graphs more smooth as expected, but when I compared the

viscosity measurements with the heat capacity curves for the same pH there was a much nicer correspondence for the low viscosity measurements than for high viscosity. So I assumed that maybe the high viscosity samples need longer time to equilibrate because the structural changes obviously are larger. Therefore I tried to decrease the scan rate further, now changing the temperature in 0.2° steps and holding it constant for 2 minutes, corresponding to a scan rate of 6° per hour. See figure 5.3 for the final results.

In figure 5.3 you see that for $pH \geq 6$ the viscosity curves have approximately the same shape and position. But for lower pH the curve shape changes and moves towards higher temperatures, the lower pH the larger shift towards higher temperatures. Furthermore the relative viscosity is much smaller for pH 3, 4 and 5.

When you zoom in (see for example figure 5.5) you see that the graphs for $pH \geq 6$ can be divided into three regions:

- **A high viscosity region** ranging from in average 19.3°C to 25.7°C with a maximum of varying size around 22°C.
- **A medium viscosity region** with a lower viscosity decreasing from up to around 1.7 to 1.1, ranging from in average 25.7°C to 30.0°C.
- **A low viscosity region** with a relative viscosity around 1.1 and close to constant, ranging from at least 5°C to the high viscosity region and from the end of the medium viscosity region to at least 50°C. The shown graphs do not all go up to 50°C but I did other measurements that do.

4.3 Fluorescence Microscopy

I used my pH 8 buffer as solvent and started at a sample temperature of 40°C. In one experiment I decreased the temperature stopping at the transition temperatures I had seen in the heat capacity profile for pH 8. It would make more sense to take pictures at 22°C where the viscosity is at max and inbetween the to last DSC peaks, but as I repeated the experiment and looked at these temperatures instead the picture was the same. The used objective is a x20 air objective. This is what I saw:
• 40°**C, above the phase transition** Vesicles of different sizes. Sausage shaped vesicles.
• 29.4°**C, third DSC peak** A lot like 40°C. A little clustering.
• 22.9°**C, second DSC peak** Still different size vesicles. A few large clusters, fewer sausage shaped vesicles.
• $19.4 - 19.5^\circ$**C, first DSC peak** The picture is now strikingly different from the other temperatures. The vesicles either changed surface structure from nice and smooth to tattered, or what we see is large clusters of tiny vesicles. This structure is seen in different sizes and shapes, sometimes also forming thin tube like structures. See figure 4.7 and 4.6.

• $15 - 10^\circ$ **C, below the phase transition** Very small vesicles. At 15°C there were still a few structures with resemblance to the phase transition structure.
• 22°**C, viscosity max** The picture is the same as around the first DSC peak.
• 26°**C, in the middle of the medium viscosity region** Only vesicles are seen.

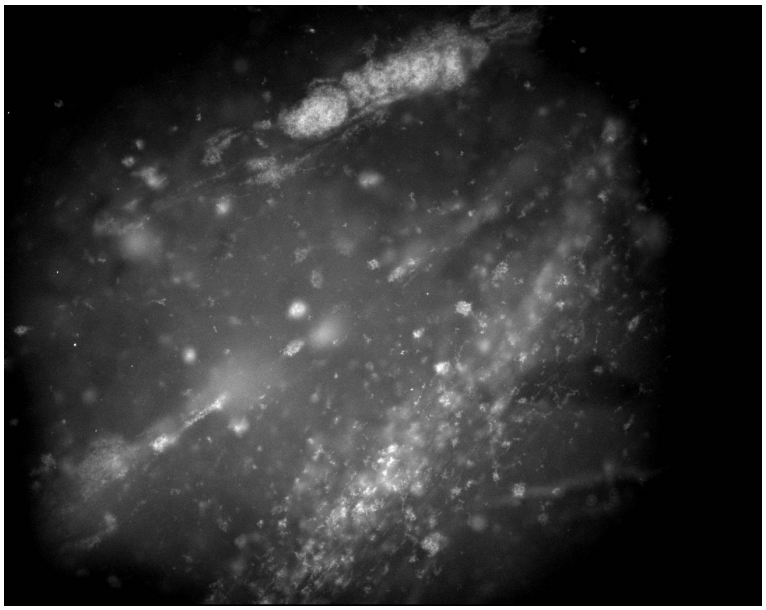

Figure 4.6: *DMPG dispersion in pH 8 buffer with 10 mM salt, $T = 19.5°C$.*

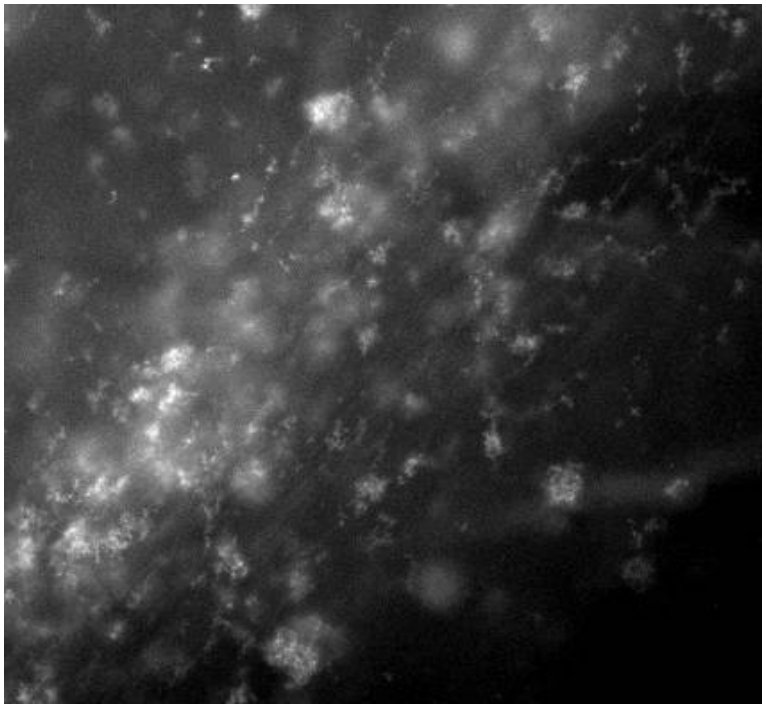

Figure 4.7: *Zooming in on figure 4.6*

Chapter 5

Discussion

5.1 pH dependence of the DSC scans

In figures 4.3 and 4.1 you see that something is clearly happening as you decrease pH below 6. As expected the behavior at decreasing pH is similar to the behavior at increasing ionic strength. When you increase the ionic strength the transition regime narrows until there is only one peak. In my measurements the width of the regime is close to constant though for pH above 5, but for pH below 6 there is only one peak in contrast to higher pH. Figure 4.3 has the shape of a titration curve. Above pH 6 the peak and boundary temperatures are close to constant (independent of pH) indicating that the membrane is close to fully deprotonated at this pH. The transition temperature is namely dependent on the surface charge density of the membrane (see theory section), which in this case thus is maybe constant above pH 6.
When the pH is decreased below 6 the transition temperature increases as expected, because protons start to attach to the lipids and the surface potential thus becomes smaller. It is not visible in the figure because I do not have points enough, but the temperatures should reach a limiting constant high value as the membranes are fully protonated. I expect this happens around pH 3, this has also been reported by others.[1]
At the pK_a of the lipid-proton binding equilibrium, the membrane is 50% protonated. If we assume that the shift in transition temperature is proportional to the surface charge density, which is proportional to one minus the protonation degree, then the pK_a is the pH where the shift in transition temperature is half of the maximum shift. This gives a pK_a of around 4. A formula showing a linear relationship between the shift in transition temperature and the surface charge density in the high potential region, is derived in the article of Träuble et al. 1976. See theory section.
Riske et al. found in 2002 that the pK_a is 4.7 for 1 mM DMPG in 6 mM NaCl. This is a little higher than my value, but I also used a higher ionic strength (up to 20 mM) which shifts the transition a little towards lower pH values because $PG - Na^+$ binding decreases the surface potential, so less work is needed to dissociate protons.[2]
My graph also possibly shows that the transition from fully protonated to deprotonated happens over approximately 2 pH units. This result is also seen in the article of Träuble et al. from 1976, although for a different charged lipid. Perhaps this narrow transition

[1] Riske et al. 2002
[2] Träuble et al. 1976

from fully protonated to deprotonated is the reason why I do not see a narrowing of the transition regime for decreasing pH as one does for increasing ionic strength.
When determining the pK_a I made some rough assumptions: The pK_a is defined for the equilibrium between two well-defined phases, the gel and fluid state of the lipid. But in this experiment we perhaps have some kind of intermediate phase. The linear relationship between temperature shift and surface charge density is derived on the basis of Gouy-Chapman theory, that is on the assumption that the membranes are planar, which they obviously are not. But this is not extremely critical, because I do not use the pK_a for calculations, but only to give qualitative descriptions.

I have with figure 4.2 shown that the enthalpy of the total melting regime is close to constant as a function of pH, except for pH 3. The cause of this is probably that the binding of protons to the head group of the lipid does not change the enthalpy much, because the main part of the enthalpy stems from the carbon chains. I got the enthalpy value 21.95 ± 0.67 kJ/mol, I estimated the uncertainty to be 10 % so it is more accurate to say approx. 22 kJ/mol. This corresponds nicely to the value given in the article of Schneider et al. 1999 which is approx. 22 kJ/mol. Riske et al.[3] measured it to be 5.7 ± 0.8 kcal/mol or 24 ± 3 kJ/mol at an ionic strength of 6 mM, 9% higher than my value.

Because the DSC scans show that for pH below 6 the processes happening when heating up the sample are irreversible and the data non-reproducible, I suspect that for low pH the lipids are changed by some kind of chemical reaction in the DSC. One possible reaction is hydrolysis of the ester bonds in the lipids. This reaction is catalyzed by the presence of acid and can cut off the carbon chains of the lipid.
It looks strange that the pH 3 sample shows a melting enthalpy that is 10 kJ larger than the other measurements, see figure 4.2. The experiment should be repeated to find out if this is a mistake. Maybe the lipid is decomposed at low pH, but the sample still consists of the same parts so the enthalpy should not change considerably.

5.2 Viscosity

5.2.1 Dependence on scan rate

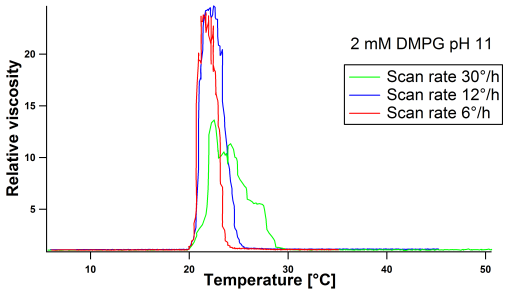

Figure 5.1: *Viscosity measurements of pH 11 samples at different scan rates.*

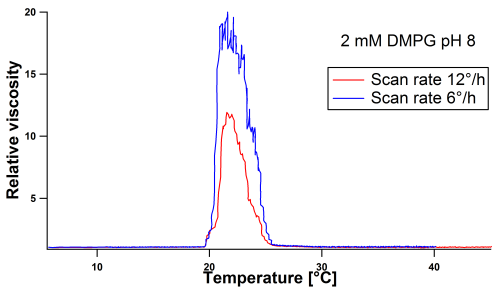

Figure 5.2: *Viscosity measurements of pH 8 samples at different scan rates.*

If you look at figure 5.1 you see that the temperature region with high viscosity narrows as the scan rate decreases. The reason for this is probably that when the sample gets more

[3] Riske et al. 2002

time to equilibrate, more structural changes or larger viscosity changes can happen within the same temperature scale. The question is then if the scan rate is low enough for the sample to fully equilibrate before the temperature is changed again. For pH 11 it looks like this might be (close to) the case. The maximal viscosity of the sample does not change significantly when decreasing the scan rate from 12 to 6° per hour. The latter scan rate is also close to the scan rate used in the DSC, which is 5° per hour and here we saw nice curves with very sharp peaks indicating that the samples had time enough to equilibrate. But I also measured pH 8, 9 and 10 with both scan rates 12 and 6°/h. Here I saw much bigger viscosities at the lower scan rate. Se figure 5.2 as an example.
Thus I am not sure if the samples with pH values below 11 fully equilibrate at a scan rate of 6°/h, and for some reason it looks like the pH 11 sample equilibrates faster than the others.

In the process of adjusting the scan rate I ran into another problem. I had problems with reproducing data for the same parameters. Sometimes I got strange measurements, that were much lower than other measurements with the same parameters and pH. One day I suspected that it might have something to do with the age of the sample. It seemed as if the lipid structures changed into a lower viscosity structure when I kept the sample in the fridge for a few days. Maybe the lipid structure collapse a little with aging. Therefore I started doing measurements only with freshly prepared samples. This improved my data and enabled me to approximately reproduce my data.
As I searched the literature my suspicion was confirmed. Kodama et al. performed measurements on DMPG samples incubated at 5°C for up to 30 days and showed that the incubation causes structural changes. Even after 1 day the DSC trace looks very different.[4].

My final data are seen in figure 5.3.

All the high viscosity curves are a little distorted, the viscosity fluctuates at the maximum. The reason for this is that at high viscosity the apparatus is very sensitive to small dislocations of the pendulum from the center. It is nearly impossible to center the pendulum perfectly, so the measurement varies a little with a period of one rotation. When the viscosity is low, the forces on the pendulum are also low. But when the viscosity is high, the forces are higher and the small periodic movement of the pendulum away from the center is intensified. I could have weakened this effect by repeating the measurements with a smaller pendulum or a smaller rotation velocity, but I did not have time enough. Instead I smoothed out the curves a little with the graphic program Igor.

5.2.2 Dependence on pH

To see if there is a connection between pH and viscosity I plotted the maximum of the smoothed relative viscosity curves (determined with the cursor) as a function of the pH. See figure 5.4. I made the error bars by first subtracting the smoothed viscosity curve from the original one for pH 6 to 11. Then I found the distance between the largest positive and the largest negative peak of this new curve and divided this by two. This is the value I used as error bar. For the lower pH I estimated the error with the cursor by looking at the fluctuations. The average relative error was $\pm 3.8\%$. But it ranged from 2.2 to 12.5

[4]K. Kodama, H. Aoki, T. Miyata, Biophys. Chem. 1999, 79, 205-217.

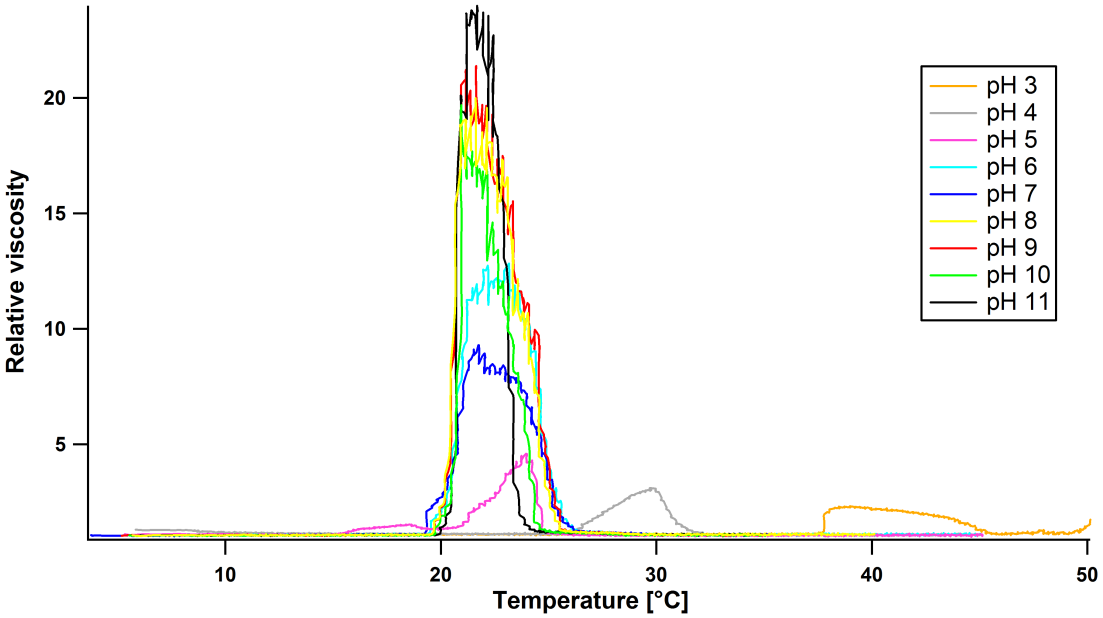

Figure 5.3: *My final viscosity measurements, all with a scan rate of 6°/h.*

%. In general it was larger for the higher viscosity. The error is not proportional to the viscosity, then the relative error should be constant. For all pH except pH 7, the graph shows that the maximum viscosity of the transition increases with pH. The graph has the same shape as the function $1-\theta(pH)$ where θ is the protonation degree. But the pK_a for this curve is about 6-7, this is higher than the pK_a for the (T, pH)-curve which was around 4. The transition here also seems to happen over a larger pH range than 2 pH units, perhaps around 3. It looks like the viscosity starts to increase as the pH rises above 4 or the pK_a of the temperature curves. But these curves indicated that the membranes are fully deprotonated for pH values above pH 6, so it is strange that the viscosity still increases until around pH 8. Thus the viscosity cannot depend on pH in the same manner as the "transition" temperatures and cannot be assumed to be proportional one minus the protonation degree as the temperatures.
The fact that there are still viscosity peaks for low pH, indicates that the intermediate phase does not disappear completely for pH below 6, as assumed in the literature.
At low pH the viscosity must not depend strongly on the protonation degree, because there is a huge difference in protonation degree when you go from pH 3 to 4, but almost no difference in viscosity. I should remember though that the nature of the transition is different for pH 3, 4 and 5, there is only one peak in the DSC profile. So maybe it is not right to compare the viscosity of the low pH samples with the higher.
The viscosity still increases from pH 6 to 8, where the membranes supposedly are fully deprotonated. So there might still be a slight change in protonation degree from pH 6 to 8. Because this change is so little but the viscosity change so obvious, the viscosity must depend much stronger on protonation degree at these higher pH values than at low pH. This could possibly be explained by comparison the the formula for the membrane potential in the high and the low potential regime respectively. But as mentioned in the theory section, the high potential approximation starts to be valid below pH 4.
What I can be sure of is that figure 5.4 shows that the viscosity increases with pH and

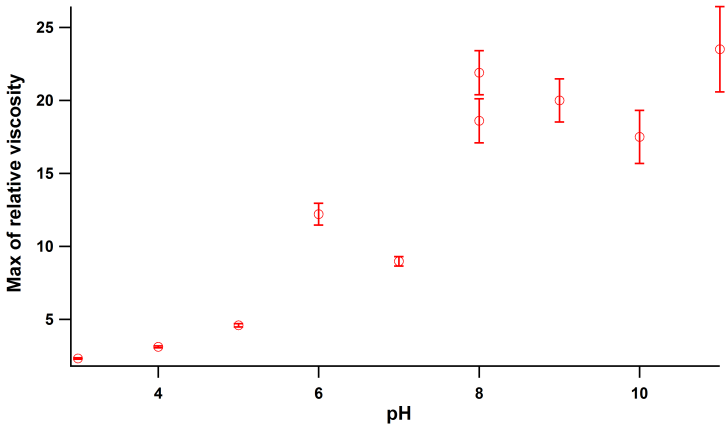

Figure 5.4: *Maxima of the viscosity curves as a function of pH.*

thus also with membrane potential until a certain limit around pH 8. Perhaps this is connected to the interaction between vesicles depending on the potential as well as the compressibility of the membranes.

The big question is of course what is the cause of the large increase in viscosity. It must be some kind of change in the structure of the lipid membranes. Maybe the structure seen in my fluorescence microscopy pictures looks like large loose aggregates of very small vesicles. Aggregation itself should maybe decrease the viscosity, because it would create larger distance between the objects. But if the structures are connected it can increase the viscosity. One possible explanation of this structure could be brownian flocculation, which happens when contacts between particles are provided by brownian motion and the primary minimum in the DLVO potential is so deep, that the attraction between vesicles is large and most of the contacts between them irreversible.[5] Riske et al. have calculated the interaction energy as a function of distance between the bilayers for different ionic strengths. They showed that there is no minimum for ionic strengths below 100 mM and thus no stable distance between the bilayers.[6] But they have done it using a temperature of 30°C, it could be interesting to see what the result is, if you do the calculations for the viscosity maximum at 22°C. Unfortunately I did not have time enough to do this.
The fact that a lack of vesicle fusion in the crossing of the intermediate phase boundaries has been shown, speaks against this theory though, because the vesicles of the supposed flocs are much smaller than the vesicles in the gel and fluid states.
Another possibility is that the pictures show perforated vesicles of different sizes and shapes. So pores form in the vesicles as in the theory of Riske et al. (see theory section). I do not find this theory unlikely because it is the most realistic on the market right now, and because it is known that membranes become softer in the transition regime (because of the increase in C_p) and therefore perhaps could form pores.
The pictures furthermore show thin tube like structures. If they are true and not just a product of flows in the sample, they could nicely explain the increase in viscosity.

[5] Soft Matter Physics, An Introduction, Kleman and Lavrentovich, 2003, page 549.
[6] Riske et al. 2007

5.3 Viscosity and Heat Capacity Curves

I have plotted the heat capacity profiles and the relative viscosity for same pH in the same figures. See figures 5.5 to 5.8 as examples. I have two viscosity axes. The viscosity axis on the left hand side is the axis of the full viscosity curve. The axis on the right hand side and the other curve I use to show what the curve looks like when you zoom in. I shifted all the viscosity curves 0.5° to the left, this gives better correspondence with the heat capacity profile. It is very likely that the thermometer in the viscometer measures temperatures that are 0.5° higher than does the DSC. Different thermometers measure the same relative changes, but not necessarily the same absolute values.

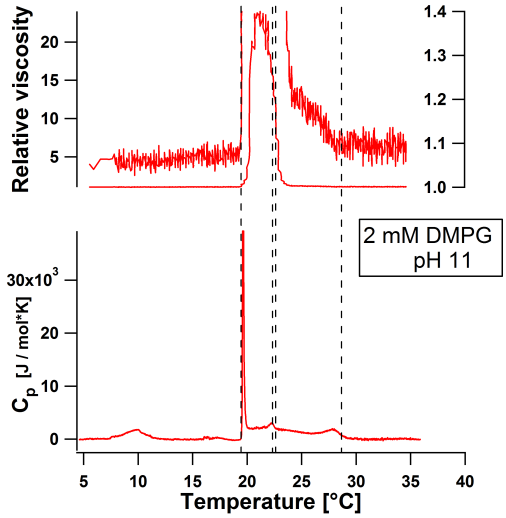

Figure 5.5: *Viscosity and heat capacity profile for pH 11. The left viscosity axis is for the full viscosity curve, the right axis and the other curve shows a zoom in of the full curve.*

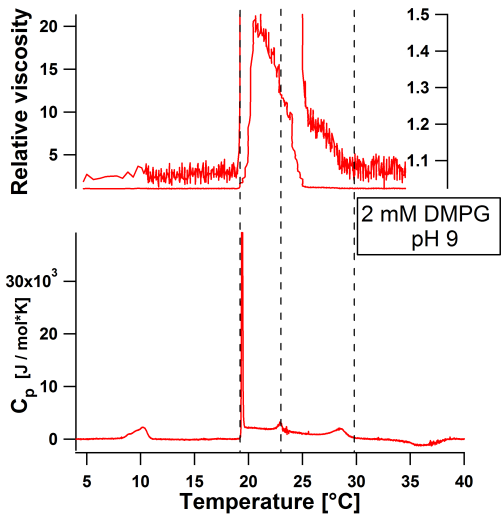

Figure 5.6: *Viscosity and heat capacity profile for pH 9. The left viscosity axis is for the full viscosity curve, the right axis and the other curve shows a zoom in of the full curve.*

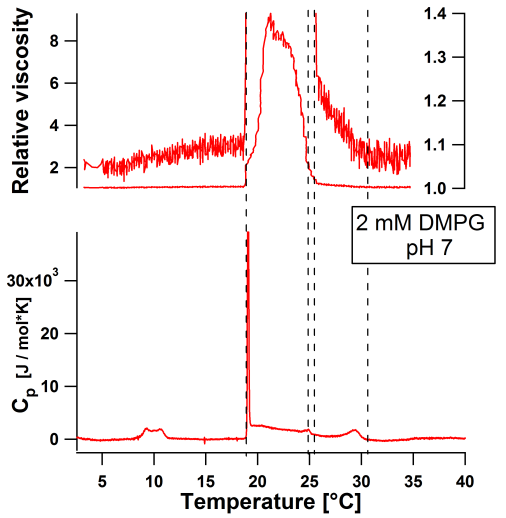

Figure 5.7: *Viscosity and heat capacity profile for pH 7. The left viscosity axis is for the full viscosity curve, the right axis and the other curve shows a zoom in of the full curve.*

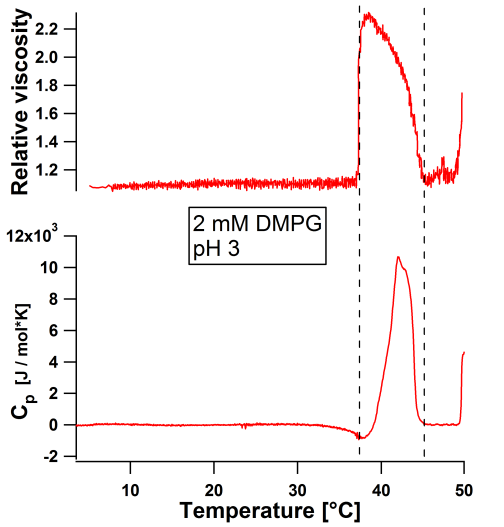

Figure 5.8: *Viscosity and heat capacity profile for pH 3. The left viscosity axis is for the full viscosity curve, the right axis and the other curve shows a zoom in of the full curve.*

All the graphs for $pH \geq 6$ show four nice connections between the heat capacity profile and the viscosity:

- The first transition peak in the DSC profile coincides with the large increase in viscosity, that is the beginning of the high viscosity phase.
- The end of the melting transition determined as the temperature where the last and third peak in the DSC profile fades out, coincides with the temperature where the viscosity decreases to a low constant value of the same size as before the transition.
- The main part of the high viscosity region is situated between the first two peaks in the C_p curve.
- The medium viscosity region starts after the second peak.

For pH 6,7 and 11 the end of the high viscosity region almost coincides with the temperature of the second peak in the DSC profile, and even better with the temperature where the second peak fades out.

For the low pH values the connection between viscosity and heat capacity is not nearly as nice, but still obvious though. The DSC profiles and the viscosity curves have approximately the same curve shape and for pH 4 and 5 some of high viscosity region falls within the beginning of the phase transition in the C_p profile, but it looks as if the two curves are shifted. If you shift the viscosity curve for pH 5 by 4 degrees to the right and for pH 4 2 degrees to the right the transition temperatures coincide much nicer. But I do not know of any effects that can shift the curves that much. For pH 3 the transitions in two graphs coincide well. And there is a strange increase in both heat capacity and viscosity starting just below 50°C.

Perhaps the fact that the regions in the heat capacity and viscosity curves do not exactly coincide is due to uncertainties in the measurement, such as lack of equilibration and a longer response time for the viscometer than for the DSC. I tried to determine the temperature boundaries of the different regions and compare them to see how well they coincide. But the numbers did not correspond very nicely with what you see in the graphs, because the uncertainty in determining the temperatures is so big. See appendix A.

So maybe figures 5.5 to 5.8 indicate that the first peak of the heat capacity profile for $pH \geq 6$ is a structural transition from a vesicular structure to a more complicated high viscosity structure. Then the second peak is maybe a transition from the high viscosity structure to some kind of vesicular structure (shown in the fluorescence microscopy) that for unknown reasons has a slightly higher viscosity than the fluid state vesicles. Finally the third peak could indicate a transition from the medium viscosity state to vesicles in the fluid state.
But if the intermediate state consists of two different structural states it should probably be visible in measurements of sample turbidity as a function of temperature. I checked this with measurements of Kinnunen et al.[7], but could not see such a change. Perhaps an indication of too high a scan rate and too few data points or an indication of my measurements being wrong.

[7] Kinnunen et al. 2007

Chapter 6

Errors

The main errors lie in the preparation of the samples and in the determination of temperatures and enthalpies of the different curves. Not in the used devices.
The error of the weight is $\pm$ 0.0001 g. The lowest weight used was around 0.0050 g (DMPG) which gives a relative uncertainty of 2 %. I calculated in the Materials and Methods section that the variation in ionic strength of the different samples is around 30 %, which gives a variation in membrane potential of only 6 %.
Determining the baseline and thus also determining the enthalpy of melting is connected with a big uncertainty, I estimated it to be around 10 %. But it is probably larger than that, because error bars showing this uncertainty do not all intersect a horisontal line made by fitting with the data points. See figure 4.2. The largest distance of a data point from the horisontal line is - 15 %.
There is a significant uncertainty in determining the temperature boundaries, because it can be difficult to estimate when a peak has ended. Appendix A shows that this is probably on the order of one degree.
Furthermore the measurement of the temperature in the viscometer is probably not exact, because the temperature is measured a little beneath the sample. This is also described in appendix A.
Finally the uncertainty of determining the maximal viscosity is 2.2 to 12.5 % because of fluctuating curves.

Chapter 7

Conclusion

I conclude that both my viscosity and DSC measurements and my fluorescence microscopy pictures indicate that the intermediate phase of DMPG can maybe be divided into two regions:

- **A high viscosity region** with a relative viscosity maximum around 22°C ranging in size from 9.0 to 23.5. At least the main part of this region falls within the region between the upper boundary of the first peak and lower boundary of the second peak in the heat capacity profile. In the microscope the structures at these temperatures look very different from the structures both in the medium viscosity region and above and below the intermediate phase.
- **A medium viscosity region** with a relative viscosity decreasing from approx. up to 1.7 to 1.1. This region starts close to just after the upper boundary of the second peak and ends with good accuracy at the upper boundary of the last peak in the heat capacity profile. Fluorescence microscopy showed single vesicles in this region and no structures similar to the structures in the high viscosity region.

This perhaps indicates that the first peak of the heat capacity profile for $pH \geq 6$ is a structural transition from a vesicular structure to a more complicated high viscosity structure. Then the second peak is maybe a transition from the high viscosity structure to some kind of vesicular structure, that for unknown reasons has a slightly higher viscosity than the fluid state vesicles. Finally the third peak could indicate a transition from the medium viscosity state to vesicles in the fluid state.
But if the intermediate state consists of two different structural states it should probably be visible in measurements of sample turbidity as a function of temperature. I checked this with measurements of Kinnunen et al.[1], but could not see such a division into regions. Perhaps an indication of too high a scan rate and too few data points or an indication of my measurements being wrong.
On the basis of my fluorescence microscopy pictures I have two suggestions for the nature of the high viscosity structure:
Maybe the structure seen in the pictures looks like large loose aggregates of very small vesicles.

[1] Kinnunen et al. 2007

Another perhaps more likely possibility is that the pictures show perforated vesicles of different sizes and shapes. So pores form in the vesicles as in the theory of Riske et al. (see theory section). I do not find this theory unlikely because it is the most realistic on the market right now, and because it is known that membranes become softer in the transition regime (because of the increase in C_p) and therefore perhaps could form pores.
The pictures furthermore show thin tube like structures. If they are true and not just a product of flows in the sample, they could nicely explain the increase in viscosity.

The DSC scans showed a clear pH dependence. For $pH \geq 6$ there is a broad transition regime with three peaks similar to what has been measured by others. The heat capacity profile nearly does not change for $pH \geq 6$, indicating that the lipids are fully deprotonated. For pH values below 6 the broad transition regime disappears and is replaced by one peak. The temperature of this peak increases with decreasing pH as expected. The pK_a of the upper and lower boundary of the melting regime vs. pH curves was found to be around 4.
Thus the effect of decreasing pH is similar to the effect of increasing ionic strength, except for the fact that at increasing ionic strength, you see a narrowing of the transition regime before it collapses into one peak. But I believe that the reason why I do not see this in my measurements, is that the transition from fully protonated to fully deprotonated happens over approximately 2 pH units, and I change the pH in steps of one.

By the use of the heat capacity profiles, I have shown that the enthalpy of the entire melting regime does not seem to depend on pH if you disregard the measurement for pH 3. But fluctuates slightly around a value of approx. 22.0 kJ/mol.

Furthermore I have shown a clear pH dependence of the maximum of the viscosity. The viscosity maximum increases with pH until around pH 8, then it stays approximately constant. The pK_a of this curve is around 6-7. So the viscosity also depends on the protonation degree and the membrane potential, but in a different manner than the DSC peak temperatures. It looks like the viscosity is only little dependent on pH for low pH up to around 4 or 5, but very dependent on protonation degree for higher pH values. The fact that there are still viscosity peaks for low pH, indicates that the intermediate phase does not disappear completely for pH values below 6.
It can be concluded from the viscosity experiments, that the viscosity increases with increasing membrane potential.

Outlook

If I had more time I would have repeated the viscosity measurements with a smaller pendulum or a lower rotation velocity, to avoid the large fluctuations in the high viscosity measurements. Perhaps I would also have tried to do the measurements with a lower scan rate to check if the samples really are fully equilibrated. But it is not possible to just keep on lowering the scan rate, because if the scan takes too long the sample will dry out. I saw that the sample dried out if I left it overnight. My scans took about 6 hours and I think that if you double that, evaporation from the sample will start becoming a problem.
Furthermore it would be a good idea to repeat the DSC scan for pH 3, to check if its enthalpy of melting really is as different from all other samples, as I measured it to be. And it could be relevant to check if the lipids are decomposed at low pH, for example by dissolving the lipid in a pH 3 buffer and then after some hours adding base to the sample

until pH has reached a value of 7. Then one could put the sample in the DSC and see whether it displays the characteristic broad transition regime. If not, something in the composition of the lipid has changed.
Finally it could be interesting to repeat the fluorescence microscopy with a much stronger objective. I took the pictures with a x20 objective, but also tried to use a x100 objective. The latter did not improve the pictures significantly.

Bibliography

[1] J. I Alakoskela and P.K.J. Kinnunen: Thermal Phase Behavior of DMPG: The Exclusion of Continuous Network and Dense Aggregates. Langmuir, Vol. 23, No. 8, pp. 4203-4213, 2007.

[2] M.T. Lamy-Freund and K.A. Riske: The peculiar thermo-structural behavior of the anionic lipid DMPG. Chemistry and Physics of Lipids 122 pp. 19-32, 2002.

[3] R.M. Fernandez, K.A. Riske, L.Q. Amaral, R. Itri, M.T. Lamy-Freund: Influence of salt on the structure of DMPG studied by SAXS and optical microscopy. Biochem. et Biophys. Acta 2007.

[4] M.F. Schneider, D. Marsh, W. Jahn, B. Kloesgen and T. Heimburg: Network formation of lipid membranes: Triggering structural transitions by chain melting. PNAS vol. 96 no. 25, 1999.

[5] K.A. Riske, L. Amaral, M.T. Lamy-Freund: Thermal transitions of DMPG bilayers in aqueous solution: SAXS structural studies. Biochim. et Biophys. Acta 1511 pp. 297-308, 2001.

[6] K.A. Riske, L. Amaral, H.G. Döbereiner and M.T. Lamy-Freund: Mesoscopic structure in the chain-melting regime of anionic phospholipid vesicles: DMPG. Biophys. Journal, vol. 86, pp. 3722-3733, 2004.

[7] H. Träuble, M. Teubner, P. Woolley and H. Eibl: Electrostatic interactions at charged lipid membranes. Effects of pH and univalent cations on membrane structure. Biophys. Chem. 4, pp. 319-342, 1976.

[8] K.A. Riske, H.-G. Döbereiner and M.T. Lamy-Freund: Gel-Fluid transition in dilute versus concentrated DMPG aqueous dispersions. J. Phys. Chem. B, 106, pp. 239-246, 2002.

[9] K.A. Riske, R.M. Fernandez, O.R. Nascimento, B.L. Bales and M.T. Lamy-Freund: DMPG gel-fluid thermal transition monitored by a phospholipid spin labeled at the acyl chain end. Chem. and Phys. of Lipids 124, pp. 69-80, 2003.

[10] K.A. Riske, M.J. Politi, W.F. Reed and M.T. Lamy-Freund: Temperature and ionic strength dependent light scattering of DMPG dispersions. Chem. and Phys. of Lipids 89, pp. 31-44, 1997.

[11] T. Heimburg: Course notes for the course "Biophysics of Membranes."

[12] R. Lipowsky and E. Sackmann: Structure and dynamics of membranes. From cells to vesicles. Elsevier 1995.

[13] M. Kleman and O.D. Lavrentovich: Soft matter physics. An introduction. Springer 2003.

[14] W. Brown and T. Poon: Introduction to Organic Chemistry. Third edition. Wiley 2005.

[15] M. K. Jain (1988): Introduction to Biological Membranes. Wiley, New York

[16] A. Hac (2003): Diffusion Processes in Membranes Containing Coexisting Domains Investigated by Fluorescence Correlation Spectroscopy Ph.d. Thesis.

Appendix A

Difference in boundary temperatures of the viscosity and heat capacity curves

Just to get a feeling of the accuracy, I made a graph of the difference between boundary temperatures in the viscosity and the heat capacity, see figure A.1. Determining the temperatures is quite uncertain though, so the numbers can only be taken as guidelines. Here I did not shift the viscosity curves by half a degree.
ΔT_{lower} is the lower boundary of the melting regime in the DSC profile minus the temperature where the high viscosity region begins.
ΔT_{upper} is the same just with the upper melting temperature and the end of the medium viscosity region.
ΔT_{mid} is the difference between the temperature of the second DSC peak and the end of the high viscosity region. And finally
ΔT_{mid2} is the difference between the upper boundary of the second DSC peak and the end of the high viscosity region.

I calculated the mean values of the different ΔT and the their standard deviation, see table

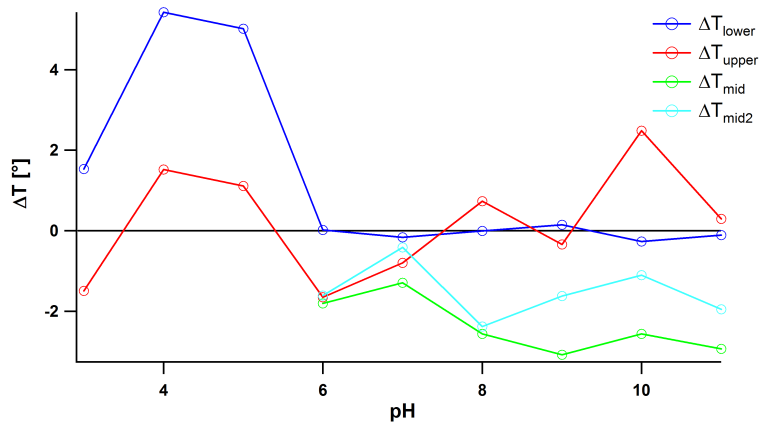

Figure A.1: *Difference in temperature boundaries of the viscosity and heat capacity profiles.*

	ΔT_{upper}	ΔT_{mid}	ΔT_{mid2}	ΔT_{lower}
$\overline{\Delta T}$	0.207°	-2.37°	-1.51°	1.29°
$\sigma_{\Delta T}$	1.32°	0.629°	1.24°	2.16°

beneath. From the table you see that the lower boundary of the melting regime and the start of the high viscosity region coincide very well. If you calculate $\overline{\Delta T_{lower}}$ for $pH \geq 6$ you get -0.063°C.

From the values of ΔT_{mid} and ΔT_{mid2} you see that the upper limit of the high viscosity region coincides better with the upper boundary of the second DSC peak than the actual peak temperature of this peak.

The table shows that the temperature differences are on the order of up to 1.5° and this difference pretty much falls within the standard deviation. So the differences can perhaps purely be due to uncertainties in the measurements and in determining the temperatures on the graphs. One possible explanation is that the viscometer has a longer response time than the DSC. In the viscometer the thermometer is not situated directly in the sample cup but a little beneath it, so the measured temperature might not be the cup temperature. The difference between cup and measured temperature increases as you move further away from room temperature, this could be the reason why ΔT_{lower} is much smaller than the other temperature differences, because the lower melting boundary and the start of the high viscosity region are around 19°C (room temperature).

Appendix B

Membrane electrostatics

About $10-40\%$ of all naturally occuring lipids are charged. They usually have one or two negative charges. The rest of the lipids are either zwitterionic (the charges in the lipid neutralize each other) or neutral. Positively charged lipids normally do not occur. The charged lipids give rise to a surface charge density σ and therefore also an electrical potential of the membrane. For a charge distribution ρ we have the following potential:

$$\Delta\Psi(r) = -\frac{\rho(r)}{\epsilon_0\epsilon} \tag{B.1}$$

Where ϵ is the relative permittivity and ϵ_0 the vacuum permittivity. When adding ions to the solution around the membrane, the ions will distribute according to a Boltzmann distribution:

$$c_i = c_{i,0}\exp\left(-\frac{z_i e\Psi(r)}{kT}\right) \tag{B.2}$$

Where i denotes the species of the ion, z is the number of charges per ion and $c_{i,0}$ is the concentration at infinite distance ($\Psi = 0$).

The charge density of the solution is given by:

$$\rho(r) = \sum_i z_i e c_i(r) \tag{B.3}$$

Thus the Laplacian of the potential can be rewritten as:

$$\Delta\Psi(r) = -\frac{1}{\epsilon_0\epsilon}\sum z_i e c_{i,0}\exp\left(-\frac{z_i e\Psi(r)}{kT}\right) \tag{B.4}$$

This equation is called the Poisson-Boltzmann equation. It can be solved numerically for given boundary conditions. But with certain assumptions one can also solve the equation analytically. The used simplified membrane model is called the Gouy-Chapman model.

B.0.1 The Gouy-Chapman Model

By assuming that the membrane surface is a plane surface with a uniform charge density and by considering the charges as point charges, one can derive a formula for the membrane potential that looks like this:

$$\Psi(x) = \Psi_0 \exp(-\kappa x) \tag{B.5}$$

Where x is the distance from the planar membrane and

$$\kappa^2 = \frac{2e^2 c_0}{\epsilon\epsilon_0 kT} \tag{B.6}$$

c_0 is called the ionic strength of the solution. It is defined as:

$$c_0 = \frac{1}{2}\sum_i z_i^2 c_{i,0} \tag{B.7}$$

- with i again being the different kinds of ions in the solution.

So the potential of a membrane in a solution with ions falls off exponentially with the distance from the membrane. Like the concentration of the ions falls off or increases exponentially with the distance depending on the sign of their charge (See eq. B.2). κ^{-1} is called the Debye length. When you look at equation B.5 you see that the Debye length is the distance from the membrane at which the potential has decreased by a factor of $1/e$ compared to $\Psi(0)$. The inverse of κ therefore gives an estimate of how big the electrostatic screening of the membrane by the ions is. The smaller Debye length, the stronger screening. Because the Debye length is proportional to $\sqrt{c_0}$, it follows that the higher ionic strength, the stronger screening. This is of course obvious as the ions are responsible for the screening.

In the Gouy-Chapman model the solution of equation B.5 is (for univalent ions, $z = 1$):

$$\Psi_0 = \frac{2kT}{e}\sinh^{-1}\left(\sqrt{\frac{1}{8\epsilon\epsilon_0 kT}}\frac{\sigma}{\sqrt{c_0}}\right) \tag{B.8}$$

Ψ_0 is the potential at the membrane surface.

By approximating the $\sinh(x)$ function you get for

- high surface potentials ($e\Psi_0 \ll 2kT$):

$$\Psi_0 = \frac{2kT}{e}\ln\left(\sigma\sqrt{\frac{1}{2\epsilon\epsilon_0 c_0 kT}}\right) \tag{B.9}$$

for $\sigma > 0$

$$\Psi_0 = \frac{2kT}{e} \ln\left(-\sigma\sqrt{\frac{1}{2\epsilon\epsilon_0 c_0 kT}}\right) \tag{B.10}$$

for $\sigma < 0$

- low surface potentials ($e\Psi_0 \ll 2kT$):

$$\Psi_0 = \frac{\sigma}{\epsilon_0 \epsilon \kappa} \tag{B.11}$$